WM41

19th International Symposium of Ballistics, 7–11 May 2001, Interlaken, Switzerland

AERO STRIPPING FROM A WATER JET

D. J. Vavrick

Naval Surface Warfare Center Dahlgren Division, Lethality and Weapons Effectiveness Branch (G24), Dahlgren, VA 22448-5100, USA

The erosion of a water jet by aero stripping was modeled using the CTH hydrodynamic computer code. The jet was assumed to be located at an altitude of 10 km and to be traveling at a velocity of 1 km/sec in air. The purpose of the simulation was to obtain information on the process of jet erosion and to help correlate analytic models. The computer model and simulation are axi-symmetric to allow finer zoning to more accurately model the erosion of the jet and the loss of the fluid by aero stripping.
The analytical model describing the behavior of the jet erosion is based on ideas of the Tate model, which models the interaction of the water and air as steady state hydrodynamic behavior. The formation of drops is axi-symmetric only so, on average, one can only expect qualitative results in this area. The calculated "drop" sizes are correlated to fluid cohesion values related to surface tension.

INTRODUCTION

Both intentional and unintentional penetration of tanks containing liquids of various kinds, especially fuels, has been an area of interest in the military for some time. Also of interest is the dynamic response of the liquid as it is expelled into the surrounding flow. Modeling of the response is made even more difficult when the flow is at high attitude and at supersonic speeds. This regime results in a configuration that is difficult to replicate in a test and to model computationally. The main reason is the relatively large time and distance scales over which this event occurs and the small time and length scales of the results of interest.

Generally, engineering models are used to predict the liquid response to the extreme loading. Currently, there is little test data at exoatmospheric altitudes from which to draw empirical data. Some models are based on data extrapolated to low pressures and high speeds. CFD computations are also lacking because of the large memory requirement to model the response of the liquid from the bulk liquid to a quasi-steady drop state. This work seeks to show a computational approach, which sheds some insight into the breakup of a liquid jet under aerodynamic loading.

METHOD

The formation of drops from a liquid jet by aero stripping was simulated using the CTH hydrodynamic computation program [1]. The jet was modeled to be a uniform stream of water of radius 3.1 cm (Fig. 1). Initially, the jet has a uniform velocity of 1 km/sec. The jet is modeled to be traveling in air, which has properties equivalent to a height of 10 km. The air has a density of 42.58 x 10^{-5} gm/cc, a pressure of 27.45 x 10^{4} dyne/cm^2 and a temperature of 0.019353 ev. The initial flow conditions are not in equilibrium so the simulation must run several hundred microseconds to become "steady state".

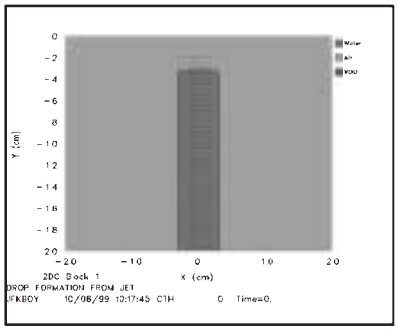

Figure 1. Initial geometry for water jet (H = 10 km, V = 1 km/sec).

The water was modeled as a Mie-Gruneisen hydrodynamic solid with minimal failure strength. The air was modeled with the air equation of state (EOS) using properties given in the SESAME Tables. These tables are really a material property database associated with the CTH code. CTH is a non-CFD (Computational Fluid Dynamics) code and, therefore, does not allow input of the fluid viscosity and surface tension. However, the artificial viscosity and failure stress will be used to approximate these quantities. The default values for the coefficients for the artificial viscosity q were used and they were $q = 0.1\,|v| + 2\,(\Delta v)^2 + 0.03\,\delta v_z/\delta r$ where $|v|$ is the absolute value of the velocity across a cell, Δv is change of the velocity across a cell and $\delta v_z/\delta r$ is the partial derivative of the axial velocity with respect to the radial coordinate. The surface tension σ was assumed related to the failure stress σ_u of the liquid.

The modeling is axi-symmetric. This allowed "zoning", which was small relative to the expected drop size. The size of a cell is 0.5 mm on a side and the zoning was uniform. The boundary conditions are reflective for the symmetric axis and transmissive for the other boundaries so the fluids can flow in and out of the boundaries. Obviously, with axi-symmetric modeling, the liquid that is stripped from the jet does not form spherical drops. Rather, the "drops" are, in actuality, rings. Therefore, these differences need to be considered when interpreting the computed results.

Tracer particles were located in rows parallel to the axis at radii spaced at mainly 0.5 cm intervals. The tracer radii locations are 0.05, 0.5, 1.0, 1.5, 2.0, and 3.0 cm. The tracers appear as black dots on the initial geometry plot (Fig. 1). The particles, which are fixed in the material, can be used to show the local properties of the material they are placed in. As

the liquid is stripped from the jet and forms drops, the tracer particles located in drops can be used to determine the environment of the drop.

The units of CTH code are metric with length in centimeters (cm), time in seconds (s) and mass in grams (gm). Some other units are given in this memo. The unit of temperature is the electron volt (ev) and is equal to 11605.33° Kelvin. Pressure has the units of dynes/cm^2 and 10^9 dyne/cm^2 is a kilobar (kb). Converted to the more familiar English unit, 1 kb equals 14,500 psi.

The analytic model that is proposed by this author to model the behavior of the jet is based on the steady state Bernoulli equation describing two impinging hydrodynamic jets.

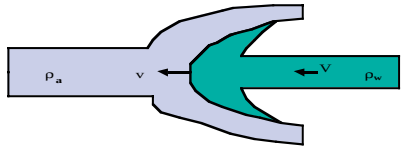

Consider a water jet of density ρ_w and velocity V moving into another fluid, air, of density ρ_a and at rest. Equating the dynamic pressure of both fluids at the stagnation point, one gets the equation,

$$\rho_w (V - v)^2 = \rho_a v^2 \tag{1}$$

where v is the interface velocity between the water and the air at the stagnation point. This equation can be solved for the tip velocity of the jet. The result is

$$v = V / (1 + \sqrt{\rho_a / \rho_w}) \tag{2}$$

If the jet cross-section is uniform and has area A, the rate at which mass is stripped away *dm/dt* is given by the expression

$$\dot{m} = \rho_w (V - v) A \tag{3}$$

If the mass that is stripped away forms into drops of the same size, i.e., diameter=D, then the rate of drop formation *dn/dt* is related to the mass rate by the expression

$$\dot{m} = \frac{\pi}{6} \rho_w D^3 \dot{n} \tag{4}$$

For the axi-symmetric simulation with non-spherical "drops", the drop diameter is determined by setting the cross-sectional area of the drop ring equal to $\pi/4\ D^2$. Then the number of drops is the total mass of the drop ring divided by a spherical drop of that diameter or

$$n = \frac{2\rho_w \pi R\left(\pi D^2 / 4\right)}{4/3 \rho_w \pi D^3 / 8} = \frac{3\pi R}{D} \tag{5}$$

Non-dimensional parameters like the Weber Number We and the Ohnesorge Number On characterize the formation of drops. Definitions for these numbers are included here for reference. The Weber number for a drop is given by the expression:

$$We = \rho_a V^2 D / \sigma \tag{6}$$

where ρ_a is the density of a air next to drop, V is the velocity of air next to drop, D is the diameter of the drop, and σ is the surface tension for the liquid.

The critical corresponding critical Weber number We_{cr} is given by the expression:

$$We_{cr} = 12 (1 + 1.077 On^{1.6}). \tag{7}$$

The Ohnesorge number is given by the expression:

$$On = \mu / (\rho D \sigma)^{1/2} \tag{8}$$

where μ is the absolute viscosity of a drop, ρ_W is the density of a drop, D is the diameter of the drop and σ is the surface tension for the liquid. Therefore, for the given conditions at the time of drop formation, D_{cr} is the diameter that satisfies eq. 6 through 8. Values for these characteristic parameters were calculated to investigate their significance.

DISCUSSION

Two water jet configurations with varying failure stresses were simulated using the CTH code. The two failure stress values, which were used, were 1 bar and 0.0001 bar. This variable was felt by the author to be correlateable to the surface tension. The surface tension s was assumed related to this ultimate or failure stress su by the equation:

$$\sigma = K \sigma_u s \tag{9}$$

where K is a correlation factor and s is the width of a modeling cell. The value of s for the configurations analyzed was 0.5 mm.

The first configuration run was with a failure stress of 1 bar. Deformed geometry with pressure contour plots are shown at two times during the 2 millisecond simulation in Fig. 2a and 2b.

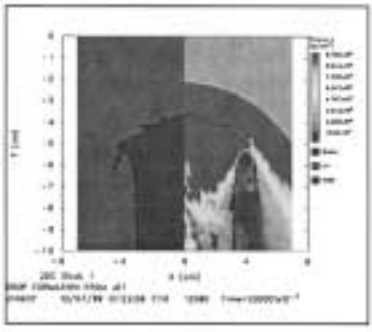

Figure 2a. Pressure contours at 1000 µsec.

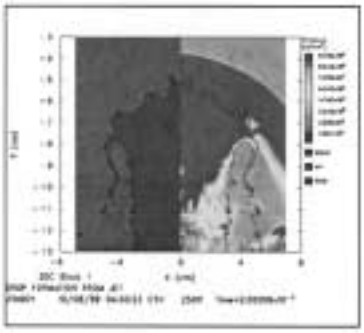

Figure 2b. Pressure contours at 2000 µsec.

The "steady" state conditions in the airflow seem to develop in a few hundred microseconds, while the "steady" state conditions in the flow of the liquid seem to take longer. The bow shock has stabilized in position by 500 μsec. The deformed shape of the air-water interface seems not stabilized by 1000 μsec. Also the rate of jet erosion, although never "constant", needs time to stabilize about the "steady state" value. No drops are seen to have been aero-stripped from the jet at 500 μsec. And when drops are formed, one notes that they are accelerated in the supersonic flow so that shocks are formed ahead of them.

The second configuration run was with a failure stress of 0.0001 bar. This change in failure stress was made in an attempt to determine what effect a change in surface tension might have for this jet configuration. Again, the steady state conditions in the airflow seem to develop in a few hundred microseconds, while the steady state conditions in the flow of the liquid seem to take longer. The rate of jet erosion can be determined by noting the location of the forward interface location between the air and the liquid as a function of time. By computing the time rate of change of the centerline location, one can create the plot of erosion rate shown in Fig 3.

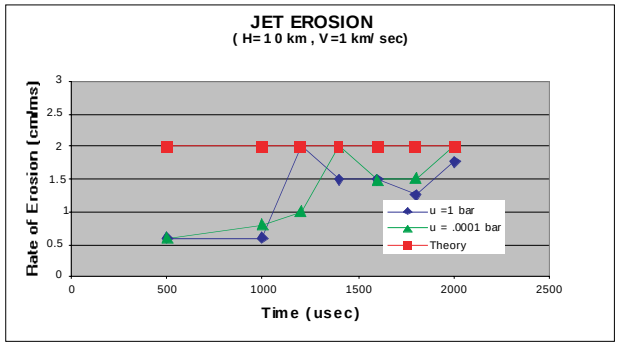

Figure 3. Jet erosion (H = 10 km, V = 1 km/sec).

Results of the simulations for the two configurations are very similar. One cannot detect visually that the higher liquid failure strength has resulted in a larger average drop size.

This conclusion is also evident from time history plots, which are obtainable at tracer point locations. Pressure, axial velocity and transverse velocity history plots are given for the outer row of tracer particles in Fig. 4a through 4c for the failure stress of 0.0001 bar.

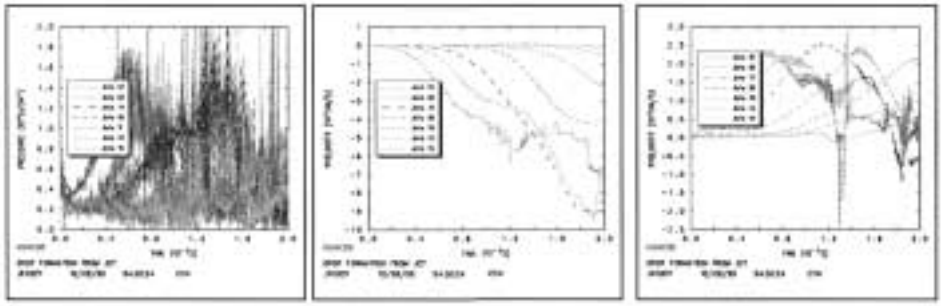

a) Pressure b) Axial velocity c) Transverse velocity

Figure 4. History plots (H= 10 km, V= 1 km/sec, σ_u=0.0001 bar).

Although the plots for the two configurations are not identical, the forces on the drops containing the tracer particles, and therefore, their accelerations and resulting velocities are very similar.

To investigate the difference in the results of the two configurations more quantitatively, enlarged geometry plots with gridding superimposed were created (Fig. 5). From these plots estimates were made of the cross-sectional area and radial location for each drop shown in the plots. Utilizing this information in a spreadsheet, an estimate was made of the volume of the drop (ring), and finally, an equivalent number of circular drops, which have the identical cross-sectional area.

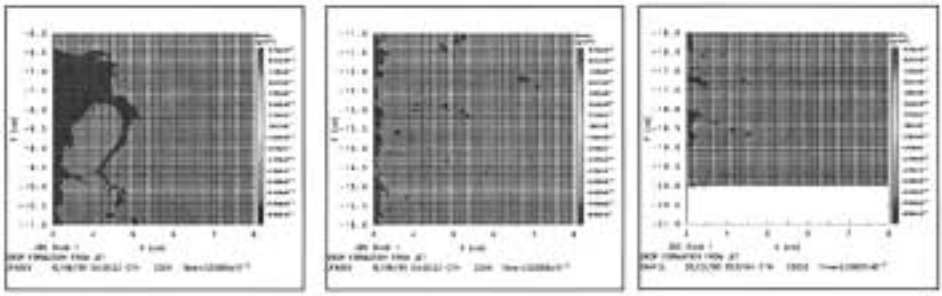

Figure 5. Drop distribution at 2000 μsec (H= 10 km, V= 1 km/sec, σ_u=0.0001 bar).

The diameters of these circular drops were also determined. The average drop size as a function of axial location is shown in Fig. 6a and 6b for the two configurations.

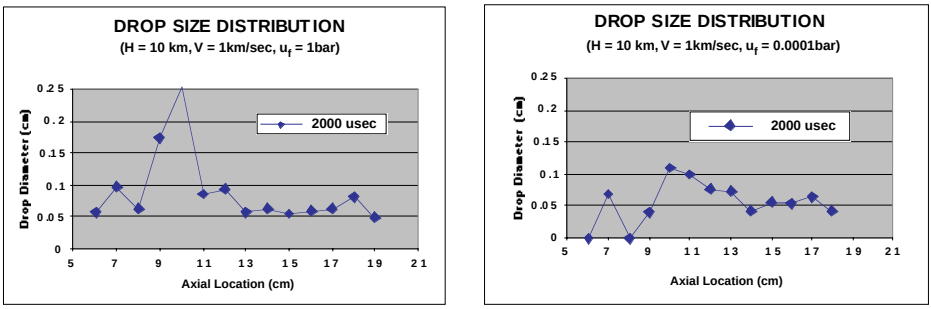

Figure 6. Drop size distribution at 2000 μsec.

After a period of drop formation and division, the drop diameter is shown on these figures to stabilize between 0.4 and 0.6 millimeters. The configuration with the higher water failure stress is slightly higher with the smaller range of 0.5 and 0.6 mm, but the difference is really within the error in estimating the area and radius. Two items are noteworthy when interpreting these results. First, this drop size is similar to the cell size, and second, the radial velocity causes an initially formed ring to decrease in cross sectional area as it expands.

The mass distribution of the drops was also computed and plotted. The total mass found in 0.5 cm length intervals along the centerline is plotted against the center location of the interval in Fig. 7a and 7b for the same two configurations. For both configurations, the largest mass is found in the region where drops are initially formed. This mass concentration is largest for the configuration with the greatest failure strength. For the configurations studied, these results indicate that an approximately 4 cm interval is required for the completion of drop formation and division. The total mass contained for each 0.25 mm diameter drop size interval over the entire jet length was also computed in the spreadsheet and plotted.

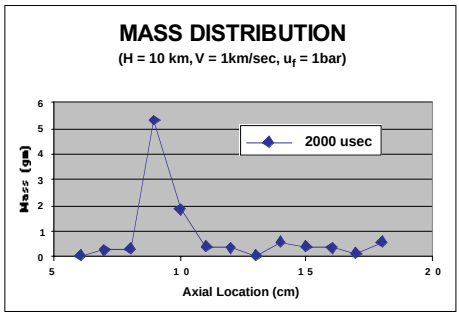

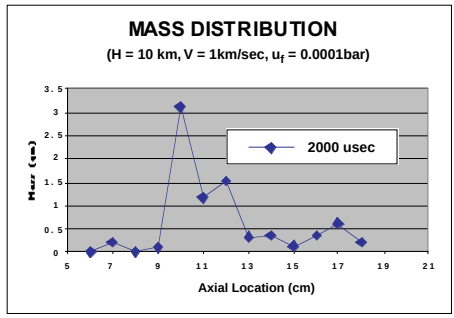

Figure 7. Mass distribution at 2000 μsec.

For the failure strength of 1 bar, the mass is concentrated in 0.5 to 0.6 mm diameter drops and in larger 2.25 to 2.75 mm diameter drops (Fig. 8a). For the lower failure strength, the mass is concentrated in 0.5 to 1.5 mm diameter drops (Fig. 8b).

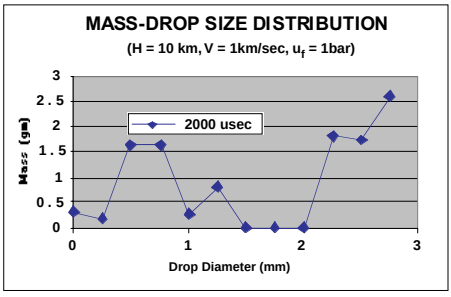

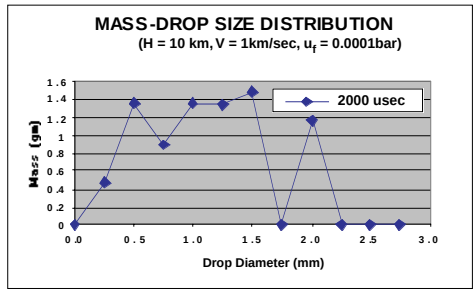

Figure 8. Mass-drop size distribution at 2000 μsec.

CONCLUSIONS

The formation and division of drops of a liquid by aero-stripping can be estimated by simulating the dynamic behavior of the liquid using the CTH hydrodynamic code. The results indicate that the drop formation process is determined primarily by the dynamic pressure gradient. A simple Tate model predicts a rate of erosion, which is approximately 30% higher than the calculated value of 1.5 cm/ms.

Similar calculations need to be pursued with three-dimensional simulations to confirm these results.

REFERENCES

1. Bell, R.L., Brannon, R.M., Elrick, M.G., Farnsworth, E.S., Hertel, etc; *USER'S MANUAL AND INPUT INSTRUCTIONS,* Version 2.0,. Sandia National Laboratories, Albuquerque, New Mexico, 19 September 1995.